scientific reports

Check for updates

OPEN

Three-dimensional characterization of hazelnut (*Corylus avellana* L.) fruit development based on X-ray micro-computed tomography

Claudio Brandoli[1,5], Laura Gargiulo[2,5], Giacomo Mele[2]✉, Claudio Todeschini[3], Elisabetta Sgarbi[1,4] & Matteo Giaccone[2]

Hazelnut (*Corylus avellana* L.) is one of the most appreciated and cultivated nuts in temperate areas. Producers are now facing an increasing demand and industries need to select high-yielding and fine-quality cultivars. In this context, a challenge to take up is the development of a rapid, non-destructive and high-resolution method to study the growth and differentiation dynamics of floral reproductive organs, to limit yield losses especially in response to climate adaptation. In this study, we scanned mixed buds from the hazelnut cultivar Tonda di Giffoni from anthesis to fruit formation by micro-computed tomography (Micro-CT). We reconstructed in three dimensions (3D) the spatial arrangement of flowers within the glomerulus, characterized the position and configuration of ovules, ovaries and funiculus as well as observed the formation of the embryo during the early developmental stages. The proposed approach enables precise volume measurements of ovaries, ovules, and embryos. It helps identify abortive ovules early and track developmental stages, such as embryo formation. Unlike traditional 2D methods, this approach captures growth patterns more accurately, supporting research on fruit development, crop quality, and genetic studies. Overall, it provides a powerful tool for advancing reproductive biology research of hazelnuts and improving hazelnut cultivation.

Keywords Plant precision phenotyping, Female flower morphology, Phenological growth stages, 3D imaging

Global hazelnut consumption has been steadily increasing for several years. Statistics from the International Nut Council estimate global production of in-shell hazelnuts to be approximately 1,400,000 tons by 2024 [1]. This rising demand has led to hazelnut cultivation spreading across all five continents, albeit predominantly in specific latitudes [2,3,4]. Concurrently to the development of this cultivation, recent years have seen significant scientific efforts have been directed toward improving hazelnut yield, with particular attention paid to floral biology, which is a critical factor in determining both productivity and nut quality[5].

Hazelnut floral biology is quite uncommon compared to other fruit-bearing trees[6], particularly due to the prolonged interval between pollination and fertilization, which can critically impact ovule growth and embryo development[6,7]. Different factors influencing fertilization success have been investigated, including pollen viability[8–10], sucrose and boron effects on pollen viability and pollen tube development[11–13], artificial pollination efficacy[3] and microclimate modifications[14].

A major challenge in hazelnut production is the high incidence of ovary abortion, leading to blank nuts. This phenomenon can vary depending on the cultivars, environmental conditions and management practices[7,15]. Over the years, the possible causes of this phenomenon have been studied. For example, fluorescence microscopy was used to understand the transport pattern of disodium fluorescein in the ovule and funiculus in order to identify any structural changes in the flower and fruit cluster[16,17]. Additionally, transcriptomic and proteomic analyses have identified molecular markers that are involved in metabolism stress response, vascular strand development, water transport and seed development which are likely associated with abortive ovary formation[18]. To better describe the developmental stages of ovary and ovules, recent microscopic studies have detailed female

[1]BIOGEST-SITEIA, University of Modena and Reggio Emilia, Via Amendola 2, 42124 Reggio Emilia, Italy. [2]Institute for Agriculture and Forest Systems in the Mediterranean (ISAFoM), National Research Council of Italy, P.le E. Fermi 1-Loc, Porto del Granatello 1, Portici 80055, Italy. [3]Ferrero Hazelnut Company, 16 Route de Trèves, Senningerberg L-2633, Luxembourg. [4]Department of Life Sciences, University of Modena and Reggio Emilia, Via Amendola 2, 42122 Reggio Emilia, Italy. [5]These authors contributed equally to this work: Claudio Brandoli and Laura Gargiulo. ✉email: giacomo.mele@cnr.it

flower and fruits development of the cultivar 'Palaz'[19], while[20] have classified fruit development stages based on embryo/kernel size.

Current studies on floral development are mainly based on photographs or optical and fluorescence microscopy[21]. Sample preparation for microscopy approach can be time-consuming requiring fixation, dehydration, cutting, use of embedding media, dyes or fluorescent markers. Moreover, the obtainable two-dimensional (2D) images allow only to observe and analyse a certain section of the tissue but cannot accurately describe the three-dimensional (3D) organization of the whole structural features. On the other hand, confocal microscopy only allows to observe three-dimensional arrangement of outer parts.

The application of X-ray micro-computed tomography (micro-CT) in the field of botany is an emerging technique to visualize the 3D internal anatomy of plant structures as a whole without the need of sample physical sectioning or preparation[22,23]. In particular, X-ray micro-CT has been recently used to analyse the internal structures of flowers in different species. For example, it allowed to identify nectar-related traits of melon flowers[24], to early determine walnut flower bud's quality[25] and to determine floral staging in barley[26].

In this context, this study aims to demonstrate the contribution that X-ray micro-CT combined with image analysis can provide to enhance the understanding of the biological mechanisms related to hazelnut development starting from the floral stage. In particular, the study describes the 3D morphological characteristics of glomeruli, ovaries and ovules at different stages of the fruit development.

Results

Preliminary observations of collected samples

The beginning of ovary growth in pollinated glomeruli was observed after the opening of the buds in the samples of the first week of April, when 9817 Growing Degree Hours were cumulated (cGDH). The ovaries then rapidly developed until the beginning of June (27215 cGDH), in concomitance with the external swelling of the cluster (Fig. 1).

The stigmas, after emergence from the bud, begin a rapid phase of extension until reaching the final length, between 3.5 and 4 mm, in seven weeks (2123 cGDH). The browning of the stigmatic tips began four weeks after anthesis (1148 cGDH), completed its evolution in 10–14 weeks (9817–17604 cGDH) until the complete necrosis of the stigmas, which began to fall from the fruit (Supplementary Fig. 1).

X-ray micro-CT imaging

The internal morphology of a mixed bud during an early stage of development, of a flower cluster after fertilization, and of nine different growth stages of the ovary sampled between 14,603 and 35,850 cGDHs have been visualised and described in detail by using X-ray micro-CT imaging and 3D image analysis.

Mixed bud

The 3D reconstruction of the glomerulus inside the bud at 1448 cGDH is reported in Fig. 2. In panel (a) it is possible to visualize the presence of the leaf primordia in the basal portion of the bud and the vascular bundle with the bracts in its middle longitudinal section. The image processing allowed to identify the structure of each individual flower, consisting of an ovary primordium with its pair of stigmas. Twelve flowers have been identified inside the analysed bud, which are shown with different colours in Fig. 2. The flowers appear arranged in pairs each located at the base of one bract in the upper part of the bud. The cross-section in panel (b) allows to observe the pairwise arrangement of the flowers, two by two on the same bract and oppositely arranged along the vascular bundle. This arrangement can be better observed in Supplementary video 1.

Flower cluster after fertilization

The 3D reconstruction of a developing fruit cluster at 12,567 cGDH with different percentages of transparency (0, 35, 70 and 100%) is shown in Fig. 3. The arrangment of the developing ovaries with their pairs of stigma as well as the size of the ovaries can be observed. It can be noted that four ovaries (average volume: 0,28 mm^3) resulted significantly smaller (t-test, df = 8, $P = 0{,}00015$) than the other six (average volume: 1,22 mm^3), arranged at different levels inside the bud: one in the upper portion, one in the middle and two in the lower portion (see arrows in Fig. 3).

Growth stages of the ovary

The internal structure development of the ovaries from 14,603 to 35,850 cGDH is shown in Fig. 4. The sample at 14,603 cGDH shows a homogeneous parenchymatous tissue without any ovular differentiation. At the apex of this ovary the base of the two stigmatic styles can be noted. Longitudinal and transversal sections of the ovary at 17,604 cGDH show the initial differentiation of the two ovules inside the parenchymatous tissue. Ovules occupy a central portion of the ovarian parenchyma taking on a flattened, lens-shaped appearance, presenting a junction with the parenchyma on opposite sides (see transversal section in Fig. 4a).

A rapid thickening of the parenchymatic tissue (endosperm) was observed in a later time, resulting in enlargement of the ovary. Ovules, originally located in a central cavity, move towards the apex of the ovary. At this stage of development and up to 19,589 cGDH, both ovules appear similar to each other in volume and shape (Figs. 4a and 5). In the sample collected at 21,429 cGDH, a beginning of differentiation appears, but not yet in ovules bulk volume. Albeit with the same size one ovule appears hollow inside, while the other retains a filled lenticular appearance.

The developing ovule (23851 cGDH) appears larger and hollow inside, while the undeveloped one retains a full lenticular appearance, remaining almost unchanged compared to the previous stage. The undeveloped ovule appears hollow only starting from 29,736 cGDH (Figs. 4b and 6).

Fig. 1. Development stages of a mixed bud and of flowers with respective fruits in the hazelnut cultivar 'Tonda di Giffoni'. The developmental stages are marked according to the cGDH scale.

The developmental embryo can be segmented at 27,215 cGDH, with a typical torpedo shape that occupies the part of the ovule connected to the funiculus. The image analysis allowed to determine also the volume of the embryo, which at this stage of development resulted of 0,01 mm^3. The 3D reconstruction at 29,736 cGDH highlights the structure of the funiculus, connected to the base of the ovary with both ovules thanks to a bifurcation just before the apex (Supplementary video 2).

From 29,736 up to 35,850 cGDH, the cotyledon embryo increases significantly in volume (5.03 mm^3) occupying the entire ovarian space (Figs. 4b and 5).

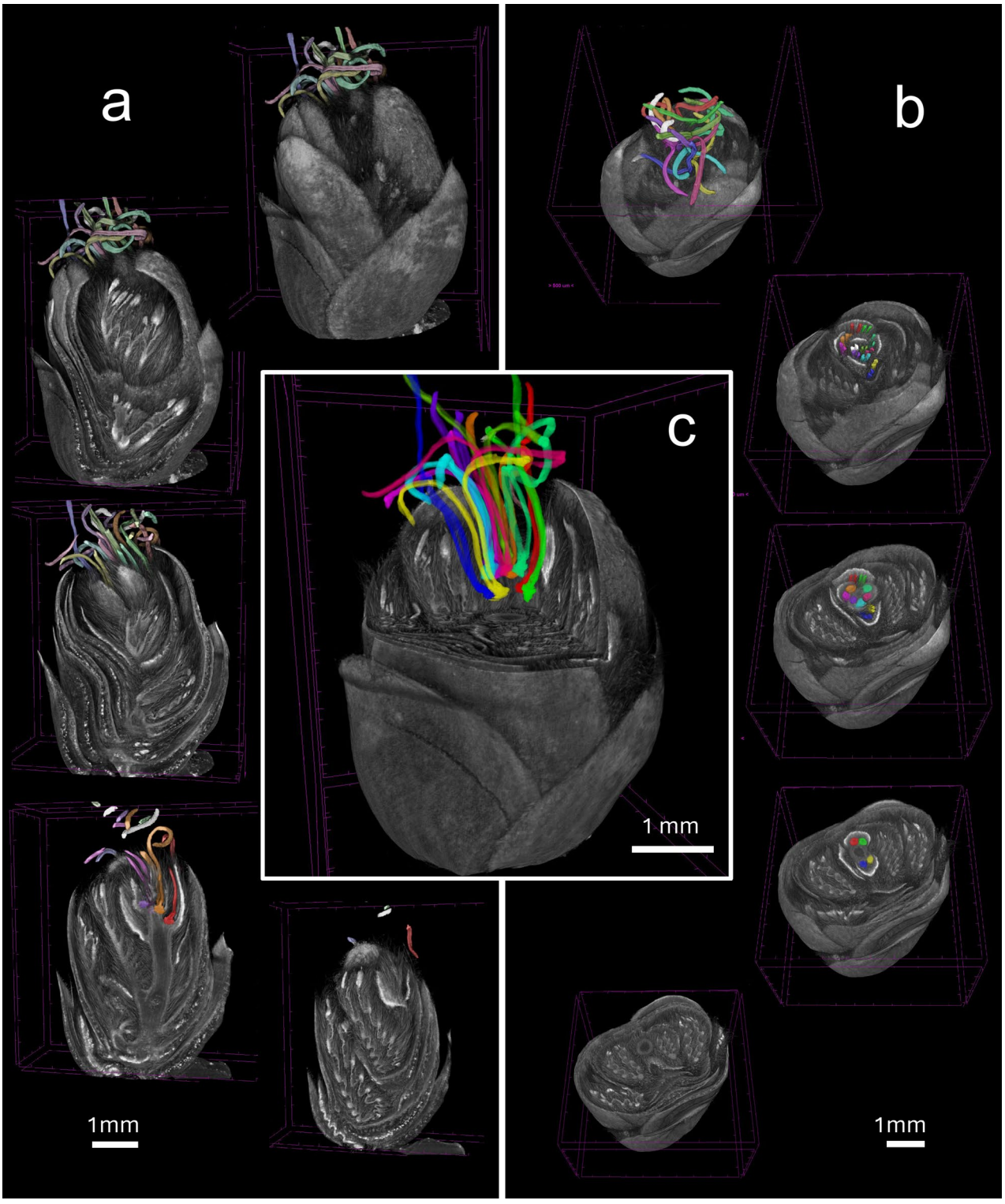

Fig. 2. Three-dimensional reconstruction of the hazelnut female bud sampled at 1448 cGDH. **a**) External structure of the bud with the stigmas and the bract primordia and sequential longitudinal sections. **b**) External structure from the apex and sequential cross sections of the bud. The single flowers (ovary primordia with pair of stigmas) are shown in different colours. **c**) The single flowers segmented inside a 3D sectioned structure of the bud.

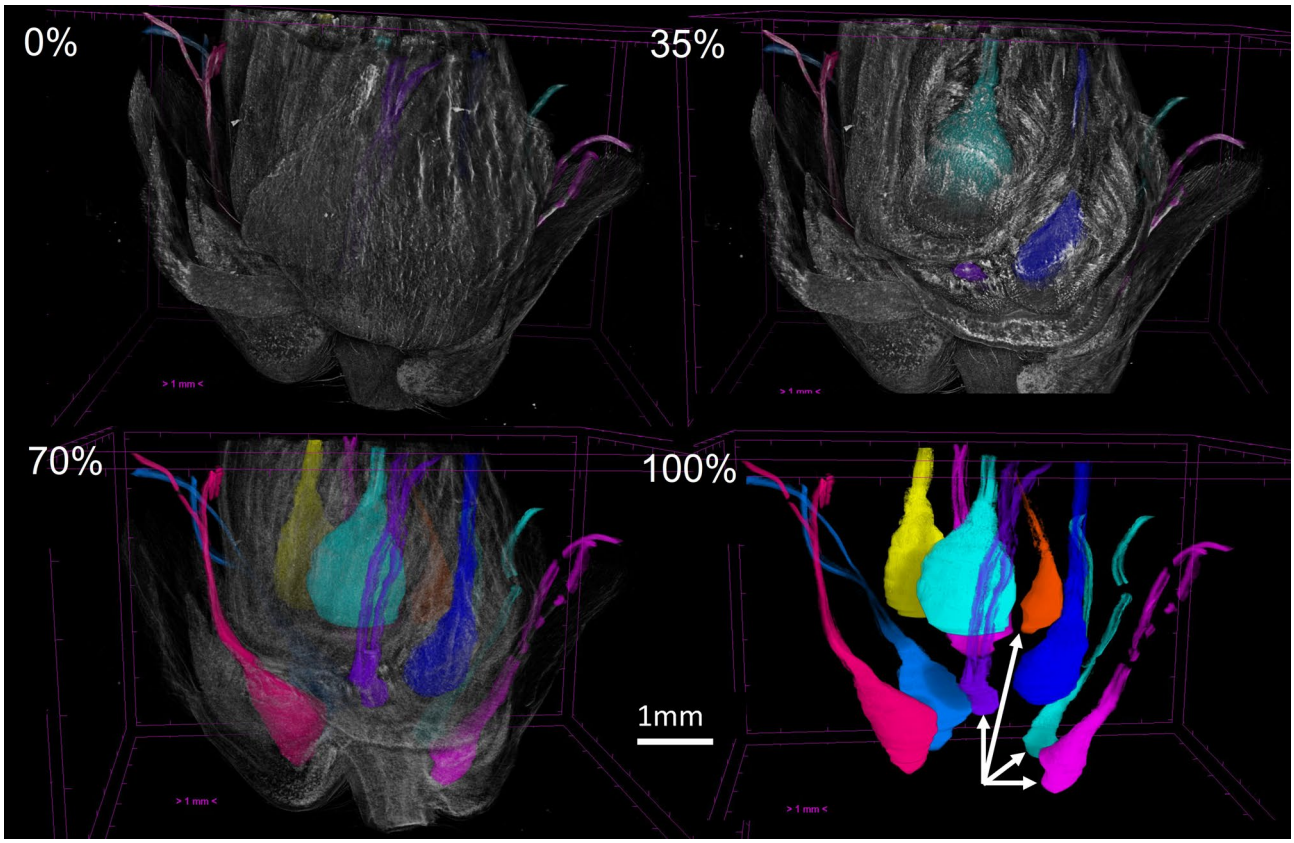

Fig. 3. 3D reconstructions of the developing fruit cluster sampled at 12,567 cGDH with different transparency percentages (0, 35, 70 and 100%). Arrows indicate significantly smaller ovaries (t-test, $P < 0.01$).

The study of the volumes among the ovary, the developing ovule and the undeveloped one, between 14,000 and 36,000 cGDH, showed a sigmoid trend, with a notable anticipation of ovarian expansion compared to that of the ovule (Fig. 5).

It can be noted that until 21,429 cGDH both ovules showed about the same small volume increase, then the developing ovule accelerated its growth respect to the undeveloped one starting from 23,851 cGDH (Fig. 5b), with a very fast increase between 29,736 and 32,702 cGDH. The undeveloped ovule maintained about the same size for the whole cGDH range. In the graph are reported also the cGHDs when embryo differentiates and completely fills the ovary.

Figure 6 summarizes the peculiar features observed at different developmental stages inside the scanned ovaries.

Discussion

In this work, we applied X-ray micro-CT combined with 3D image analysis to samples of mixed buds, flower and fruit clusters, with a particular attention to developing ovaries in order to be able to characterize the arrangement of the female reproductive structures of the hazelnut as a whole. Although the structure of ovary primordia was previously visualised and described in histological sections by e.g.,[17,27,28] and in a stereomicroscope study by[19], the proposed approach allows to observe the overall 3D spatial organization of all the inner parts of the hazelnut female bud and of the developing fruit cluster. Moreover, it allows to perform accurate volume measurements of ovaries, ovules, embryos and, potentially, of each visualized structure inside the female reproductive organs.

In particular, as the technique allows observation of the internal structure of both the developing fruit cluster and the ovules, it lets an early identification of which ovaries are putatively abortive in the fruit cluster (Fig. 3) and which of the two ovules in the ovary is the developing one. In fact, it can be seen that a cavity (the earliest observed differentiation in the ovules) develops in one of the two ovules before their size differentiation (Figs. 4a and 5). A cavity was also observed in the undeveloped ovule only after the differentiation of the embryo in the developing one (Figs. 4b and 6).

As shown in Fig. 4, it was possible to observe the funiculus and its spatial relationship with the ovule, starting from the sample collected at 23,851 cGDH[16]. visualized the disodium fluorescein transport in funiculus and developing ovule during hazelnut fruit development using a light microscopy approach. The technique used in this work could support such type of studies to better understand the 3D spatial organization of both funiculus and ovules at different developmental stages and contribute to study the mechanisms of ovary abortion. This

Fig. 4. Longitudinal sections of 3D reconstructions of the hazelnut ovary at different developmental stages. Numbers in the figure indicate the different cGDH. Longitudinal sections (only for 17604 cGDH is reported also the transversal section) show the different tissues in false colours: the ovary is in brown, the developing ovule in red, the undeveloped ovule in green, the embryo in yellow and the funiculus in white. Panel b) shows more details of the apex of the ovary (in grey) and the 3D structure of the embryo (yellow), virtually separated from the developed ovule (red).

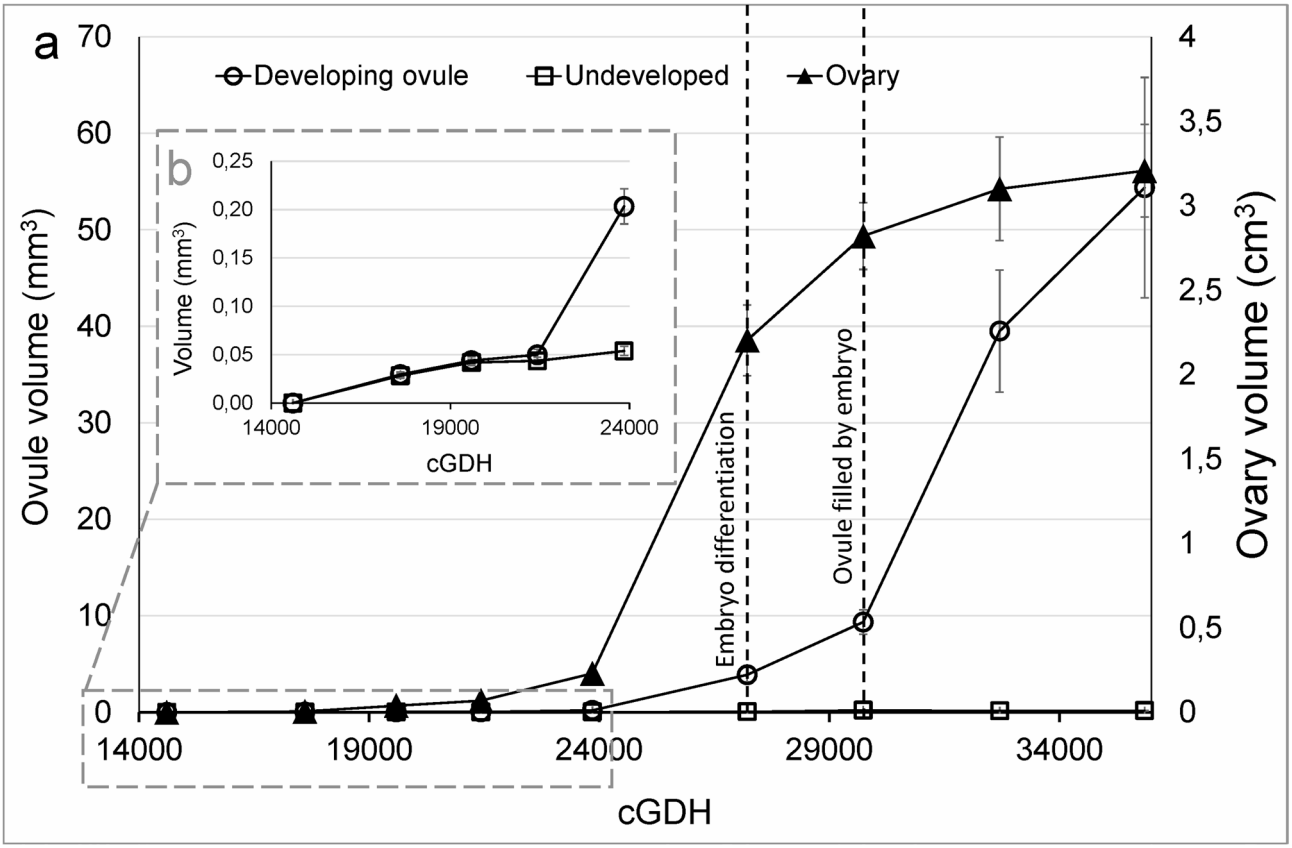

Fig. 5. Volumetric development of the ovaries ($n = 3$) and their developing and undeveloped ovules. The two vertical dotted lines indicate the cGDH values when the embryo differentiation inside the developing ovule was detected (left line) and when the complete filling of the developing ovule by the embryo was observed (right line). b) Ovules volume zoomed scale between 14000 and 24000 cGDH. Error bars represent standard deviations.

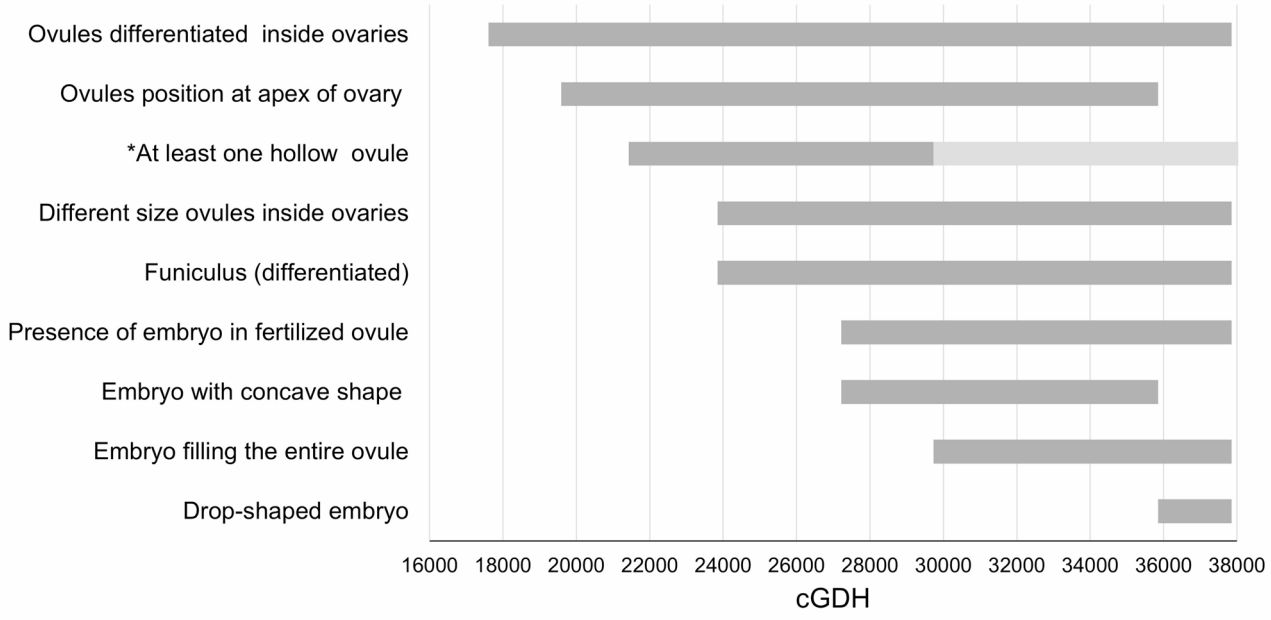

Fig. 6. Features development inside the hazelnut ovaries observed according to the cumulated GDH. *After 29,736 cGDH (light grey bar) the hollow ovule is the undeveloped one.

could be useful, as well, to better understanding the origin of phenomena like double kernel that can affect the crop quality.

The image segmentation of the embryo inside the developed ovule was possible starting from the sample collected at 23,851 cGDH while in the ovaries sampled at 27,215 cGDH and at 29,736 cGDH (see Fig. 4b) the embryos seem to correspond to the stage III (early torpedo embryo) and stage V (embryo with cotyledons), respectively, as defined by[5]. These referments are based on the classical histological approach and related to 2D sections.

The graphs of ovary and ovule volume growth (Fig. 5) look sigmoid curves, as observed in previous works e.g.,[7,16], although in such works the size was based on linear measurements. In particular, we observed that the embryo was formed when the rate of ovarian development began to decline (27215 cGDH) and the ovule growth rapidly increased only after it was filled by embryo.

Overall considered, the proposed approach can contribute to better follow the phenological growth stages of the female buds during flowering, until now described only based on external aspects e.g.,[29]. More generally, this technique provides also an effective way for the 3D visualization of flowers and fruits and could therefore contribute to collect big data for the construction of 'digital fruit trees', as defined by[30] and the development of useful technologies of agricultural interest[25]. Moreover, it has the potential to contribute to studies on genetic and molecular mechanisms of ovary differentiation and development e.g.,[31,32] or studies on shade nets and influence of light spectra on nut development e.g.,[14].

Despite the limitations due to image resolution, which does not allow tissues to be observe on a cell scale as in histological sections, the approach of X-ray micro-CT and 3D image analysis can certainly offer valuable support in both research and industry, simplifying the study and monitoring of the sequence of phases during the flowering and growth of hazelnut fruits.

Methods

Plant material and sampling

The early flowering hazelnut (*Corylus avellana* L.) cultivar "Tonda di Giffoni" was considered for this study. Samplings were carried out weekly since the last week of December, 2022 till the last week of July, 2023 from the hazelnut collection field belonging to the Università Cattolica del Sacro Cuore - DI.PRO.VE.S. (Emilia Romagna Region, Italy), only from the long fruiting branches of 6-year-old plants, excluding short and sylleptic branches. Shrubs were grown according to the multi-stem bush model, planted at a distance of 5 × 4; conventional horticultural care for field management, pruning, plant protection, irrigation and plant nutrition, was provided, according to the traditional techniques for commercial hazelnut production. According to the extended BBCH reference scale described by[33], the collected buds ranged from the red dot stage (code 600) until the appearance of future fruits on 51–100% of the flowers (code 695). Successively, clusters were collected from their appearance until the shell and kernel reached 100% of their final size (code 799) and the nuts separated from the husk at the basal scar and began to fall freely (code 89). Five to six buds and four fruit clusters were selected from at least three different shrubs and in different portions of the canopy for each developmental stage. After the selection of the buds, the branches were cut and carefully transported to the laboratory in order to avoid any possible damage to the protruding stigmas.

Permission has been obtained from the Università Cattolica del Sacro Cuore of Piacenza to collect Corylus avellana L. plant material.

Meteorological data and growing degree hours calculation

Hourly meteorological data were recorded using the on-site Davis Instruments® station (model Vantage VUE) (https://davisinstruments.com/). Then, the "Cumulate growing degree hours" (cGDH), a weighted measure of the heat accumulation to which a tree is exposed, were determined. The cGDH corresponding to each sampling time were calculated according to ASYMCUR model described in[34], assuming a condition of plant stress absence. The calculation started on December 21 st at 23:00 GMT, when the chilling requirement of 640 h was met according to[35] for female flowers of "Tonda di Giffoni" hazelnut variety. In Supplementary Table 1 the correspondence between dates and cGDH is provided.

Microscopic observation of buds, flowers and fruit clusters

For each sampling stage, 5–6 mixed buds, each composed by 10–16 flowers, were observed under a Nikon SMZ800 stereomicroscope equipped with a DS-Fi2 high-definition camera (Nikon Instruments Inc.). Furthermore, we observed single flowers after the external bracts had been manually removed, isolating the ovary primordia with stigmas. The images obtained were used to digitally measure the stigmas length and the progression of tissue senescence (browning), from the tip to the base of all stigmas, using the Fiji-ImageJ software (https://imagej.net/). The colorimetric evaluation of the progressive stigmatic browning was performed according to the protocol of[36]. Data were expressed as percentages of color variation (supplementary Table 2).

X-ray microtomography and image processing

The 3D morphological characteristics of glomeruli, ovaries and ovules, selected at different stages of development, were scanned using X-ray microtomography technique and analysed. Namely, the glomeruli were scanned at the beginning of the browning process of the stigmas (1448 cGDH), the ovaries and ovules from the beginning of the fruit cluster development (12567 cGDH) till 35,850 cGDH. X-ray micro-CT scans were performed at the Institute for Agriculture and Forestry Systems in the Mediterranean - National Research Council of Italy (Portici, Italy) using the desktop microtomograph Bruker Skyscan 1272 (Bruker, Belgium). The microtomograph is equipped with a cone beam X-ray source adjustable in the 20–100 kV energy range and allows to analyse a cylindrical volume of 6.5 cm in diameter and 7.2 cm in height as maximum sample size.

			cGDH									
		1448	12,567	14,603	17,604	19,589	21,429	23,851	27,215	29,736	32,702	35,850
Acquisition	Source Voltage (kV)	50	40	40	50	50	60	60	60	60	60	70
	Source Current (μA)	200	200	250	200	200	166	166	166	166	166	142
	Rotation Step (deg)	0,2	0,2	0,4	0,2	0,2	0,2	0,2	0,2	0,2	0,2	0,4
	Filter (mm)	no	no	no	no	no	Al 0,25	Al 0,25	Al 0,25	Al 0,25	Al 0,25	Al 0,50
	Distance sample to source (mm)	36,74	60,00	23,74	36,72	55,07	52,50	64,05	150,01	101,31	101,31	201,78
	Image Pixel Size (μm)	2	4	1,24	2	2,99	3,49	5,49	9,99	8,70	8,70	16,49
	Scan duration (min)	89	98	32	98	96	113	106	162	105	105	91
Reconstruction	Phase Retrieval	Yes (δ/β = 1000)*	no	no	Yes (δ/β = 1000)*	no	no	no	no	no	no	no
	Ring artefact correction (%)	0	10	20	10	20	20	20	20	20	20	20
	N° of reconstructed sections	1809	1630	951	1529	1203	1191	1186	1596	1634	1549	1090
	Reconstruction duration per slice (seconds)	0,316	0,116	0,228	0,056	0,079	0,116	0,127	0,074	0,089	0,290	0,044

Table 1. Image acquisition and reconstruction parameters set for each sample. *δ/β is a tuning parameter of the phase retrieval algorithm of Paganin et al. (2004).

Samples of buds, fruit clusters and single ovaries were held on a very thin cylindrical support using an orthodontic wax (Sunstar Europe S.A., Switzerland) with low X-ray attenuation coefficient and then positioned on the rotating stage. Image acquisition was set using different combinations of source voltage and source current based on the developmental stage of the samples due to the different size and density of the tissues. The optimal parameters used for scanning and image reconstruction for each growth stage are reported in Table 1.

Before the 3D reconstruction, if needed, the single-distance phase-retrieval algorithm described by[37] was applied to the CT projection images, to enhance the tissue contrast. Then cross-section images were reconstructed using NRecon version 2.2.0.6 software (Bruker, Belgium) obtaining a 3D reconstruction of the acquired samples.

After 3D image reconstruction of the bud and the fruit cluster, all ovary primordia with their pair of stigmas were segmented binarizing the grey-level images of their volumes of interest (VOIs). Similarly, the grey-level images of the scanned ovaries and their ovules were binarized. Finally, the volumes of three ovaries and their ovules at each considered developmental stage were measured (supplementary Table 3). Otsu method was applied to identify the binarization thresholds[38]. The image processing and analysis were performed using CTAn v.1.23.0.2 software.

Statistics

Statistical differences of stigma lengths and percentages of stigma necrosis (browning) between samples of each collection stage were assessed using ANOVA and Tukey's test using SPSS software version 28.1.1 (https://www.ibm.com/products/spss-statistics). Welch's two-tails *t*-test was used to evaluate volume differences among ovary groups in the fruit cluster after applying Levene's test to assess homoscedasticity of the compared groups (Excel: https://www.microsoft.com/en-us/microsoft-365/excel).

Data availability

No datasets were generated or analysed during the current study.

Received: 31 May 2025; Accepted: 22 August 2025
Published online: 02 October 2025

References

1. International Nut & Dried Fruit Council (INC). Hazelnuts Global Statistical Review. (2024). https://inc.nutfruit.org/hazelnuts-global-statistical-review-3/ (accessed 24 February 2025).
2. Bastias, R., & Grau, P. (2004, June). Floral phenology of commercial cultivars and Chilean pollinizers of hazelnut (Corylus avellana L.) in Chile. In VI International Congress on Hazelnut 686 (pp. 151-156). https://doi.org/10.17660/ActaHortic.2005.686.19
3. Ascari, L. D. Guastella, M. Sigwebela, G. Engelbrecht, O. Stubbs, D. Hills, T. De Gregorio, C. Siniscalco (2018)'Artificial pollination on hazelnut in South Africa: preliminary data and perspectives', Acta Horticulturae, (1226), pp. 141–148. Available at: https://doi.org/10.17660/ActaHortic.2018.1226.20.Baldwin, B., & Guisard, Y. (2012, March). The status and future challenges for the Australian hazelnut industry. In VIII International Congress on Hazelnut 1052 (pp. 321-327). https://doi.org/10.17660/ActaHortic.2014.1052.45
4. Baldwin, B. & Guisard, Y. The status an future challenges for the Australian hazelnut industry. *Acta Hortic.* **1052**, 321–327. https://doi.org/10.17660/ActaHortic.2014.1052.4 (2014).
5. Beyhan, N. & Marangoz, D. An investigation of the relationship between reproductive growth and yield loss in hazelnut. *Sci. Hort.* **113** (2), 208–215 (2007).
6. Germain, E. The reproduction of hazelnut (Corylus avellana L.): a review. III International Congress on Hazelnut, Acta Horticulturae, No. 351, Alba (CN), Italy, September 14–18, pp. 195–209. (1994).
7. Liu, J. F., Cheng, Y. Q., Yan, K., Liu, Q. & Wang, Z. W. The relationship between reproductive growth and blank fruit formation in *Corylus heterophylla* fisch. *Scientia Horticolturae*. **136**, 128–134 (2012).
8. Ellena, M. et al. Preliminary results of supplementary pollination on hazelnut in South Chile. *Acta Hort.* **1052**, 121–127. https://doi.org/10.17660/ActaHortic.2014.1052.15 (2014).

9. Novara, C. et al. Viability and germinability in long term storage of Corylus avellana pollen, Scientia Horticulturae, 214, pp. 295–303. (2017). Available at: https://doi.org/10.1016/j.scienta.2016.11.042
10. Balık, H. İ. & Arif, T. M. Impact of Varying Storage Temperatures on Hazelnut (Corylus avellana L.) Pollen Quality, Applied Fruit Science, 66(6), pp. 2287–2294. (2024). Available at: https://doi.org/10.1007/s10341-024-01209-2
11. Brandoli, C., Cristofori, V., Silvestri, C., Todeschini, C. & Sgarbi, E. The development of an improved medium for the in vitro germination of Corylus Avellana L. Pollen. *Forests* **15** (7), 1095. https://doi.org/10.3390/f15071095 (2024a).
12. Brandoli, C. Mortada, A., Todeschini, C. et al.(2024b) The role of sucrose in maintaining pollen viability and germinability in Corylus avellana L.: a possible strategy to cope with climate variability, Protoplasma [Preprint]. Available at: https://doi.org/10.1007/s00709-024-02015-z
13. Pannico, A. et al. Foliar nutrition influences yield, nut quality and kernel composition in hazelnut Cv Mortarella. *Plants* **12** (11). https://doi.org/10.3390/plants12112219 (2023).
14. Guastella, D. et al. Effect of Photo-Selective Shade Nets on Pollination Process and Nut Development of *Corylus avellana* L., Frontiers in Plant Science, 11, p. 602766. (2020). Available at: https://doi.org/10.3389/fpls.2020.602766
15. Dong, Y. et al. Obstacles in sugar transportation lead to blank nut formation in Hazel (*Corylus heterophylla*). *Ind. Crops Prod.* **224**, 120365. https://doi.org/10.1016/j.indcrop.2024.120365 (2025).
16. Liu, J., Cheng, Y., Liu, C., Zhang, C. & Wang, Z. Temporal changes of disodium fluorescein transport in hazelnut during fruit development stage. *Sci. Hort.* **150**, 348–353. https://doi.org/10.1016/j.scienta.2012.12.001 (2013).
17. Liu, J. et al. Comparison of ultrastructure, pollen tube growth pattern and starch content in developing and abortive ovaries during the progamic phase in Hazel. *Front. Plant Sci.* **5**, 528 (2014).
18. Liu, J., Xing, J., Fang, J., Ai, P. & Cheng, Y. New insight into ovary abortion during ovary development of hazelnut through a combined proteomic and transcriptomic analysis. *Sci. Hort.* **234**, 36–48. https://doi.org/10.1016/j.scienta.2012.01.008 (2018).
19. Akçin, Y. Stages of Female Flower and Fruit Development in 'Palaz'Hazelnut Cultivar Grown in Ordu, Türkiye. Applied Fruit Science, 67(2), 71. (2025). Available at: https://doi.org/10.1007/s10341-025-01300-2
20. de Benedetta, F. et al. Fruit phenology of two Hazelnut cultivars and incidence of damage by Halyomorpha Halys in treated and untreated Hazel groves. *Horticulturae* **9** (6), 727 (2023).
21. Riechmann, J. L. & Ferrándiz, C. (eds). Flower development: methods and protocols (Vol. 2686). Springer Nature. (2023). https://doi.org/10.1007/978-1-0716-3299-4
22. Karahara, I., Yamauchi, D., Uesugi, K. & Mineyuki, Y. Three-dimensional visualization of plant tissues and organs by X-ray micro–computed tomography. *Microscopy* **72** (4), 310–325 (2023).
23. Piovesan, A., Vancauwenberghe, V., Van De Looverbosch, T., Verboven, P. & Nicolaï, B. X-ray computed tomography for 3D plant imaging. *Trends Plant Sci.* **26** (11), 1171–1185 (2021).
24. Begot, L. et al. Precision phenotyping of nectar-related traits using x-ray micro computed tomography. *Cells* **11** (21), 3452 (2022).
25. Gao, Z. Three-dimensional virtual flower bud of walnut tree based on micro-computed tomography. *Agron. J.* **114** (4), 1935–1943 (2021).
26. Tracy, S. R., Gómez, J. F., Sturrock, C. J., Wilson, Z. A. & Ferguson, A. C. Non-destructive determination of floral staging in cereals using X-ray micro computed tomography (μCT). *Plant. Methods.* **13** (1), 9. https://doi.org/10.1186/s13007-017-0162-x (2017).
27. Wei, H. et al. Genome-wide identification of the ARF gene family and ARF3 target genes regulating ovary initiation in Hazel via chip sequencing. *Front. Plant Sci.* **12**, 715820 (2021).
28. Liu, J., Zhang, H., Cheng, Y., Kafkas, S. & Güney, M. Pistillate flower development and pollen tube growth mode during the delayed fertilization stage in *Corylus heterophylla* fisch. *Plant. Reprod.* **27** (3), 145–152. https://doi.org/10.1007/s00497-014-0248-9 (2014a).
29. Paradinas, A. et al. Phenological growth stages of 'barcelona'hazelnut (Corylus Avellana L.) described using an extended BBCH scale. *Sci. Hort.* **296**, 110902 (2022).
30. Grisafi, F. et al. Modelling the architecture of hazelnut (Corylus avellana) Tonda Di Giffoni over two successive years. *Silico Plants.* **6** (1), diae004. https://doi.org/10.1093/insilicoplants/diae004 (2024).
31. Cheng, Y., Zhang, Y., Liu, C., Ai, P. & Liu, J. Identification of genes regulating ovary differentiation after pollination in Hazel by comparative transcriptome analysis. *BMC Plant. Biol.* **18**, 84. https://doi.org/10.1186/s12870-018-1296-3 (2018).
32. Cheng, Y., Mou, Y., Zhang, X., Liu, C. & Liu, J. iTRAQ protein profiling reveals candidate proteins regulating ovary and ovule differentiation in pistillate inflorescences after pollination in Hazel. *Tree. Genet. Genomes*. **15** (2), 21. https://doi.org/10.1007/s11295-019-1328-7 (2019).
33. Taghavi, T., Rahemi, A. & Suarez, E. 'Development of a uniform phenology scale (BBCH) in hazelnuts', Scientia Horticulturae, 296, p. 110837. (2022). Available at: https://doi.org/10.1016/j.scienta.2021.110837
34. Anderson, J. L., Richardson, E. A. & Kesner, C. D. Validation of chill unit and flower bud phenology models for 'Montmorency' sour cherry. In I International Symposium on Computer Modelling in Fruit Research and Orchard Management 184 (pp. 71–78). (1986).
35. Mehlenbacher, S. A. Chilling requirements of hazelnut cultivars. *Sci. Hort.* **47** (3–4), 271–282 (1991).
36. Ross, J. Microscopy New Zealand Incorporated Fiji Workshop 2017, The university of Auckland. (2017). Available at: https://www.fmhs.auckland.ac.nz/en/sms/about/our-departments/biomedical-imaging-research-unit/image-processing-and-analysis/mnz-workshop-2017.html (Accessed: 11 November 2024).
37. Paganin, D., Gureyev, T. E., Pavlov, K. M., Lewis, R. A. & Kitchen, M. Phase retrieval using coherent imaging systems with linear transfer functions. *Opt. Commun.* **234**, 87–105 (2004).
38. Otsu, N. A threshold selection method from gray-level histograms. *IEEE Trans. Syst. Man. Cybern.* **9** (1), 62–66. https://doi.org/10.1109/TSMC.1979.4310076 (1979).

Acknowledgements

Authors thank the Hazelnut Company division of the Ferrero Group for their collaboration and contribution and Prof. Sergio Tombesi of the Università Cattolica del Sacro Cuore of Piacenza for authorizing access and sampling of the plant material analysed.

Author contributions

Conceptualization: Claudio Brandoli, Claudio Todeschini; Methodology: Laura Gargiulo, Giacomo Mele; Formal analysis: Claudio Brandoli, Laura Gargiulo, Giacomo Mele; Investigation: Claudio Brandoli, Laura Gargiulo, Giacomo Mele, Matteo Giaccone; Data curation: Laura Gargiulo, Giacomo Mele; Writing—original draft: Claudio Brandoli, Laura Gargiulo, Giacomo Mele; Writing—review & editing: Claudio Brandoli, Laura Gargiulo, Giacomo Mele, Matteo Giaccone, Claudio Todeschini, Elisabetta Sgarbi; Visualization: Claudio Brandoli, Laura Gargiulo, Giacomo Mele; Supervision: Claudio Brandoli, Giacomo Mele, Elisabetta Sgarbi; Project administration: Elisabetta Sgarbi, Giacomo Mele; Funding acquisition: Elisabetta Sgarbi, Giacomo Mele.

Funding
This work was supported by FERRERO TRADING LUX S.A. (1) project "Characterizing male and female sterility in hazelnut cultivars" and (2) project "3D imaging of hazelnut reproductive structures".

Declarations

Competing interests
The authors declare no competing interests.

Additional information
Supplementary Information The online version contains supplementary material available at https://doi.org/10.1038/s41598-025-17344-z.

Correspondence and requests for materials should be addressed to G.M.

Reprints and permissions information is available at www.nature.com/reprints.

Publisher's note Springer Nature remains neutral with regard to jurisdictional claims in published maps and institutional affiliations.